Surface Radiation Budget and Climate Classification

G. LOUIS SMITH
Virginia Polytechnic Institute and State University, Blacksburg, Virginia

ANNE C. WILBER AND SHASHI K. GUPTA
Analytical Services and Material, Inc., Hampton, Virginia

PAUL W. STACKHOUSE JR.
Atmospheric Sciences Division, NASA Langley Research Center, Hampton, Virginia

(Manuscript received 26 February 2001, in final form 20 September 2001)

ABSTRACT

The surface radiation budget of a region is strongly tied to its climate. An 8-yr climatology of surface radiation budget components for 2.5° regions over the earth is examined in order to learn how the regional climate and surface radiation are related. The yearly cycles of a few individual regions were studied by plotting monthly mean net longwave flux as a function of net shortwave flux at the surface. These plots show trajectories that are characteristic of the climate class. The behavior of the trajectories of surface radiation and their relation to the regional climate can be understood with simple conceptual models for many cases.

From an examination of these trajectories, a set of parameters is developed, such as mean net longwave flux and range of net shortwave flux, which distinguish various climate classes on the basis of the surface radiation. These criteria are applied to produce a map of regional climate classes based on surface radiation, similar to those of Koeppen or Trewartha and Horn, which were based on vegetation, temperature, and precipitation. The current maps can be used to explore the relationships between surface radiation and regional climate.

1. Introduction

The climate and surface radiation budget (SRB) of a region are intimately related. An examination of the yearly cycle of SRB of the regions of various climate classes shows that the yearly cycle of SRB is a characteristic of the climate class. Because of the wide variation of climate over the earth, methods have been developed for classifying regional climate for millennia (Sanderson 1999). The first modern climate classification scheme is that of Koeppen and Geiger (1936), who developed his method over a period of decades, starting as early as 1900. His method was based on the vegetation types of a region, together with temperature and precipitation. Haurwitz and Austin (1944) state that ''the main purpose of classification of climate is to provide a reasonably easy and logical guide that permits a comprehensive survey of the great variety of climatic types.'' Haurwitz and Austin explain climate in terms of air masses and relate them to Koeppen's classification. Koeppen's classification has been the starting point of other methods which have since been developed, notably that of Trewartha and Horn (1980), hereafter referred to as TH80. The TH80 method is based on temperature and precipitation alone, without reference to vegetation. This change of basis results in a change of nomenclature, for example, rain forest becomes tropical wet, savanna becomes tropical wet/dry, desert becomes arid, and steppe becomes semiarid. Terjung (1970) used the presatellite surface radiation estimates of Budyko (1958) to develop a climate classification scheme based on net radiation at the surface.

TH80 state that the purpose of climate classification is to introduce simplicity and order, so as to facilitate analysis and explanation. Barrett (1974) points out that the aim of climate classification is a reasonable representation of climatic reality. He further states that it should be kept in mind what the purpose of the scheme is, the types of available data, and ''the contemporary level of relevant atmospheric concepts.''

An 8-yr surface radiation budget dataset has been developed due to the demand of researchers (e.g., Ramanathan 1986) based on satellite measurements (Darnell et al. 1992; Gupta et al. 1992; Gupta 1999). This dataset provides monthly mean surface radiation components for regions defined by the International Satellite

Corresponding author address: Dr. G. Louis Smith, NASA Langley Research Center, Mail Stop 420, Hampton, VA 23681-2199.
E-mail: g.l.smith@larc.nasa.gov

Cloud Climatology Project (ISCCP) grid (Rossow and Schiffer 1991), which is a quasi-equal area grid of 2.5° latitude by 2.5° longitude at the equator and covers the globe with 6596 regions. The dataset is for the period, July 1983–June 1991 and includes mean net longwave (LW) radiation and shortwave (SW) radiation for each calendar month for each region.

This paper uses the recently published SRB dataset (Gupta et al. 1999) in order to study the relation between a region's climate and its SRB components. Our approach is quite a bit different from that of Terjung (1970), who used only the total net radiation. We use net SW and net LW fluxes as separate parameters. A brief description of the SRB dataset and the definitions of different SRB parameters used in the following discussion is presented in the next section. In the following sections, we then examine the SRB of regions of various climate classes and note the characteristics of the yearly cycles of each. It is demonstrated that SRB can be used to duplicate the climate classification of TH80 by use of very simple criteria. The purpose of this demonstration is to begin to show relationships between regional climate and SRB in terms of climate classes. Finally, histograms are used to examine some properties of the full set of 6596 regions.

2. SRB dataset description

An 8-yr SRB dataset of monthly average SW and LW surface radiative fluxes has been developed recently (Gupta et al. 1999) using parameterized radiation models (Darnell et al. 1992; Gupta et al. 1992) and meteorological inputs available from the ISCCP (Rossow and Schiffer 1991). Spatially, the fluxes were computed on the quasi-equal area ISCCP grid that is 2.5° × 2.5° at the equator and covers the globe with 6596 regions. Temporally, the fluxes were computed first on a daily average basis, permitting a full accounting of the diurnal variation. The daily averages were then used to compute monthly means. The period covered by the dataset is from July 1983 to June 1991. This dataset is available online to the science community worldwide from the NASA Langley Atmospheric Sciences Data Center [Baum and Barkstrom (1993); http://eosweb.larc.nasa.gov.]

Net SW and LW fluxes are generally defined as downward flux minus upward flux, and net total flux as net SW flux plus net LW flux. By these definitions, net SW flux is always positive (or zero) and represents a warming of the surface, while net LW flux is mostly negative and represents a cooling of the surface. In order to facilitate the discussion of the main theme of this paper, we have made a slight departure with regard to the sign of the net LW flux. We decided to treat net LW flux as a positive quantity. With this choice, 70 W m^{-2} will be referred to as larger value of net LW flux than 60 W m^{-2}, and that makes the discussion more intuitive because 70 W m^{-2} represents a larger cooling of the surface than 60 W m^{-2}. Under this convention, the net total flux will be defined as net SW flux minus net LW flux, thus providing correct magnitude and sign.

The fluxes of this dataset were compared extensively with measurements from a number of surface sites. Many of these comparisons were subject to the spatial mismatch problem that arises when point measurements are compared with gridbox averages representing much larger areas. For those comparisons, where several measurement sites were located within a grid box, biases for monthly averages were <10 W m^{-2} and rms differences in the 10–15 W m^{-2} range for both SW and LW fluxes. For a detailed discussion of the fluxes and the errors in the dataset, the reader is referred to Gupta et al. (1999).

3. Yearly cycles of net longwave and shortwave radiation

In this paper only the monthly mean net longwave radiation flux (NLW) and monthly mean net shortwave flux (NSW) are considered. A few regions were selected as representative of various climatological regions, whose locations are shown in Fig. 1. The climatological mean value is computed for each calendar month of the 8-yr dataset. For the selected regions, NLW is plotted as a function of NSW for each month of the year in Fig. 2 to show the yearly cycle of net radiation at the surface. Because NLW is negative if it cools the surface, for points below the NLW = NSW line, the absolute value of NLW is less than NSW, so that the surface is heated by radiation. For points above the NLW = NSW line, the surface is cooled by radiation. For land surfaces, the heat storage is small for a monthly mean, so this surplus (deficit) is transferred to (from) the atmosphere as sensible or latent heat. For ocean regions, surplus energy may be also stored or advected away by currents, or if there is a deficit of radiant energy the ocean may cool locally or advect energy into the region. In analogy to plots with velocity components as axes, which are used by dynamicists, we call these plots SRB hodographs.

The trajectories of surface radiation for various regions in Fig. 2 are distinguished by the line and symbols codes. The January point is indicated by ★ for each site. The region over Winnipeg, Canada (center at 51.25°N, 114°W) was selected as a temperate continental region. During January the insolation at the top of the atmosphere (TOA) and surface is small. As the sun moves northward during the spring and summer the surface NSW increases. The NLW also increases slightly as the surface warms. During fall the curve is only slightly above the curve for spring, due to the slight lag of temperature behind radiative heating. This case for a high-latitude continental climate is almost linear. The yearly cycle consists of the annual cycle, the semiannual cycle, and higher harmonics. If NSW and NLW have annual cycles only, the SRB hodograph will be an el-

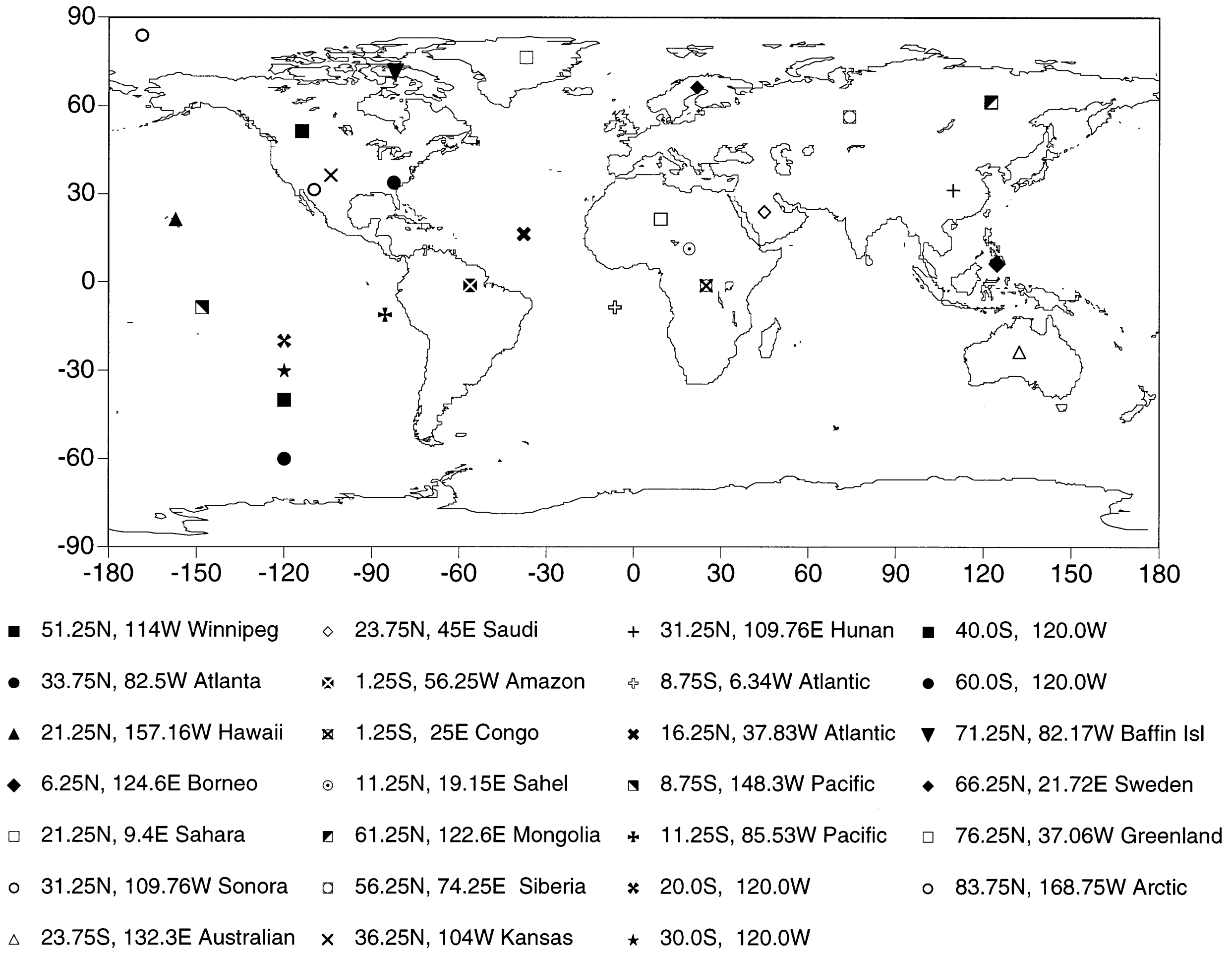

FIG. 1. Map showing locations of regions.

lipse. If NSW and NLW are in phase, the ellipse will reduce to a straight line segment. Case 2 is for a low-latitude eastern continental region over Atlanta, Georgia. Beginning in January, as the insolation and NSW increase, the NLW increases slowly until April, after which the NLW decreases due to increased humidity until August. By October the trajectory has returned to the line described in winter. The maximum NLW is in April and the minimum is in August, giving a range of 27 W m^{-2}. Thus, this low-latitude (33.75°) eastern continental case has a linear form with a clockwise loop during the summer. The presence of this loop indicates a semiannual cycle and is associated with the change in circulation in flow pattern induced by the semipermanent Azores (or Bermuda) high during warm weather.

Case 3 is for Hawaii, which at 21.25°N, 157.16°W is an oceanic subtropical locale. The NSW has a range of 130 W m^{-2} due to the yearly cycle of solar declination but the NLW varies over a total range of only 11 W m^{-2}. Case 4 shows the surface budget for the region centered at 6.25°N, 124.62°E, which is near Borneo and is a deep convective region. This region has a very small range in both NSW and NLW. For the Hawaii and Borneo cases, the NSW is large because of the low albedo of the ocean surface. The Sahara Desert is case 5. The NLW is between 70 and 120 W m^{-2} and is the highest noted thus far. The very low humidity of the desert permits the large upwelling longwave radiation from the high-temperature surface to pass through the atmosphere without a matching large downwelling longwave radiation from the atmosphere. The NSW is not as large as the Hawaii case because of the high surface albedo of the desert. Thus the loci of monthly means for various regions occur in different parts of the NSW–NLW plane, which depend on the climatological influences such as solar radiation, humidity, cloudiness, and surface type.

Figure 3 is a SRB hodograph of some tropical and subtropical regions. Desert regions have been selected from the Sahara, Sonora, Australian, and the Empty Quarter of the Saudi Desert. All of these deserts have NLW above 60 W m^{-2} and NSW between 100 and 260 W m^{-2} so that they cluster in one part of the NSW–NLW domain. Charney (1975) explains that deserts maintain themselves by a feedback in which rain is pre-

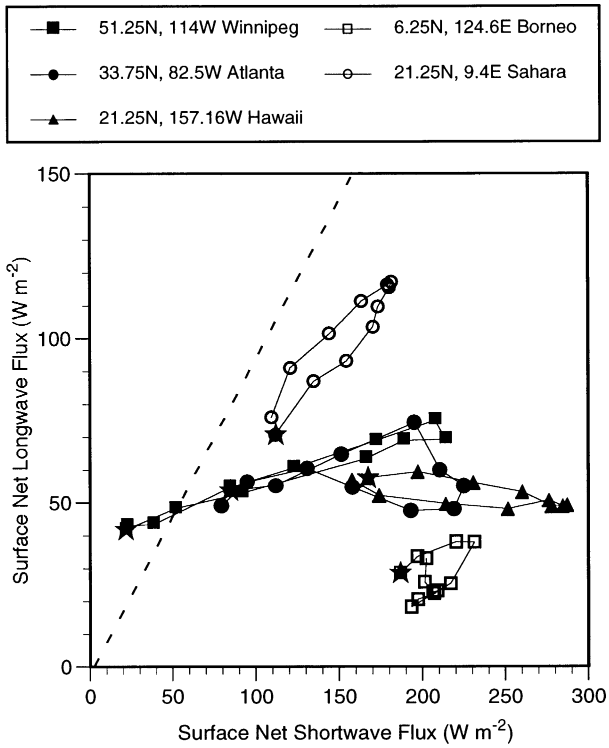

FIG. 2. Annual trajectory of NLW and NSW at surface for Winnipeg, Atlanta, Hawaii, Sahara, and Borneo. Jan is indicated by ★ for each site.

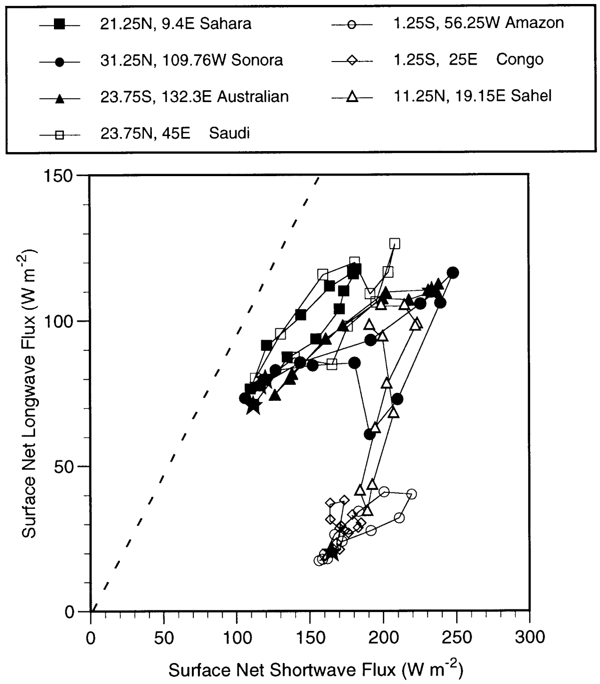

FIG. 3. Annual trajectory of NLW and NSW at surface for desert, deep convection, and savanna regions. Jan is indicated by ★ for each site.

vented by subsidence of dry air. This subsidence is due to radiative cooling of the air above the desert and results in an outflow at lower levels, thereby preventing moist air from entering the region. The subsidence also suppresses clouds, so there is little downward longwave flux from the dry air and the NLW is quite large.

Figure 3 also shows deep convective regions in the Amazon (1.25°S, 56.25°W) and Congo Basins (6.25°S, 26.43°E). These regions have NLW between 17 and 41 W m^{-2} and NSW between 156 and 219 W m^{-2}. The NLW is low due to cloud cover and high humidity, both of which inhibit upward LW and increase downward LW. Neelin and Held (1987) explain the requirement of a surplus of radiative energy to provide the latent heat flux necessary to maintain deep convection. This surplus at the surface is given by the distance of a point below the NLW = NSW line and is the largest of all areas shown here. Thus in the Tropics the clouds and high humidity of a deep convective region provide a radiative feedback that assures the continuation of the radiative surplus, thereby maintaining the stability of the system.

In addition to deserts and deep convective regions, Fig. 3 shows a region in the Sahel of Africa centered at 11.25°N, 19.15°E. In January the NLW has its maximum of 105 W m^{-2} and decreases to its minimum of 34 W m^{-2} in August. The deep convective region of equatorial Africa migrates during the year, following the sun northward to this region in July–September to bring the rainy season. By October the deep convection has moved southward, leaving this region to have its dry season. In January, during the dry season, the NLW is typical of a desert. In August, during the rainy season, the NLW is typical of a deep convective region. The NSW is between 189 and 224 W m^{-2} throughout the year. Thus, the trajectory moves from the part of the NSW–NLW domain that is characteristic of a desert to the part that is characteristic of a deep convection region, with a corresponding change in weather. The figure 8 aspect of the trajectory is due to a very strong annual cycle of NLW and a semiannual cycle dominating the NSW, caused by the sun passing over this latitude twice each year. A region south of the Congo Basin at 6.25°S, 26.43°E shows a similar behavior but with a small yearly change in NLW. This region has the maximum NLW in July and minimum in December. Because it is south of the equator, this region is six months out of phase with the Sahel region.

Figure 4 shows some continental regions in the midlatitudes. These sites are in western Siberia, Mongolia, Hunan (Central China), and Kansas. The Georgia and Saskatchewan trajectories are repeated. During the year each of these regions has a large range of NSW, 100–200 W m^{-2}, but a much smaller range of NLW, 20–40 W m^{-2}. Although the NSW for several regions exceed the desert cases for some months, the NLW is much lower for these cases than for deserts.

Figure 5 shows SRB hodographs of some high-latitude land and ice-covered regions. Within the Arctic

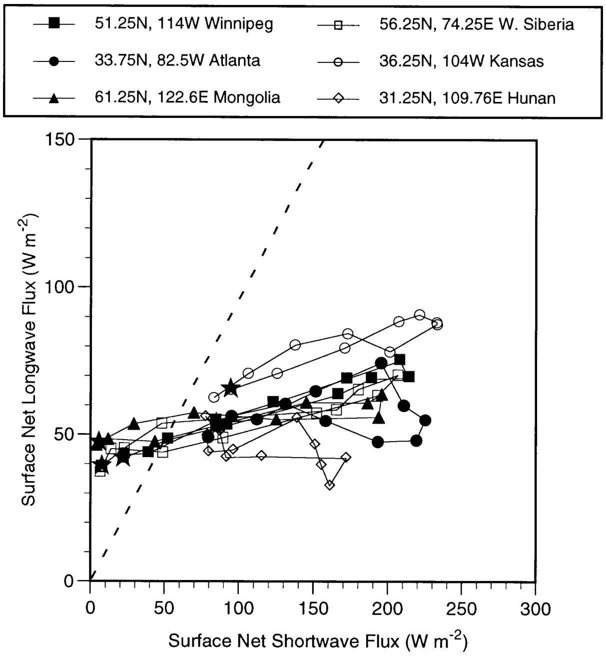

FIG. 4. Annual trajectory of NLW and NSW at surface for midlatitude continental regions. Jan is indicated by ★ for each site.

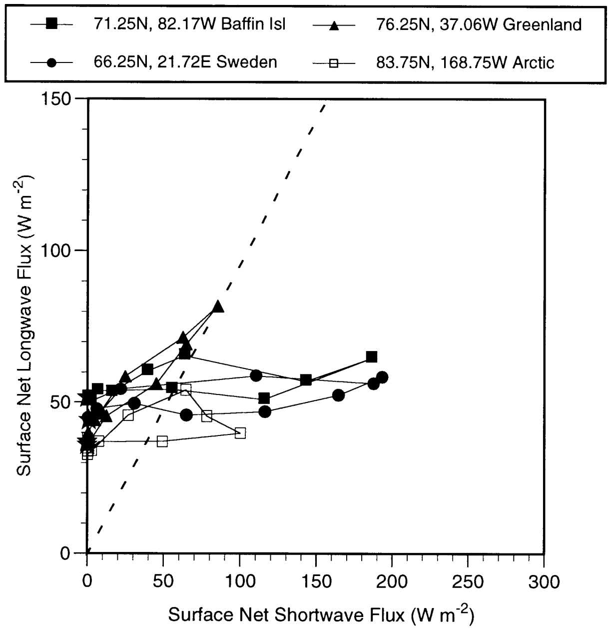

FIG. 5. Annual trajectory of NLW and NSW at surface for high-latitude land and ice-covered regions. Jan is indicated by ★ for each site.

and Antarctic Circles, there is no insolation for some period during winter, the length of this period being longer as one approaches the Poles. The trajectory is shown for a region of the Arctic Ocean (83.75°N, 168.75°W). While NSW = 0, the NLW is less than 40 W m^{-2}. Because of the high albedo and low solar elevation, the maximum NSW is less than 100 W m^{-2}. During the Arctic night, the surface is cooled by NLW and there is no insolation, so the surface must be heated by transfer of sensible heat from the planetary boundary layer. Similar considerations apply to Greenland, also shown. However, for Greenland the NLW rises to 80 W m^{-2} during summer. The trajectories for Baffin Island and Sweden cover a wider range of NSW, though not a wider range of NLW. The Baffin Island region is within the Arctic Circle (71.25°N, 82.17°W) and the Sweden region is barely south of the Arctic Circle. Because they are not snow covered during summer, the surface albedo of these regions is lower than for Greenland and the Arctic Ocean and the maximum NSW exceeds 180 W m^{-2}.

Tropical ocean SRB trajectories are shown by Fig. 6. The NLW is less than 60 W m^{-2} for all regions shown here, but is as high as 85 W m^{-2} for some subtropical oceanic regions. The NSW is between 140 and 300 W m^{-2}. Because of the immense heat-storage capacity of the ocean and the small yearly temperature change in these regions, most of the variation of NLW must be due to changes of cloud cover and humidity. These changes in turn are linked to larger-scale changes with season. Higher-latitude ocean regions are shown in Fig. 7. These sites are in the South Pacific Ocean at longitude 120°W and latitudes 20°S, 30°S, 40°S, and 60°S. Although the NSW goes through a large yearly cycle, the NLW varies little through the year at each location. Outside the Tropics, the NLW decreases slightly as

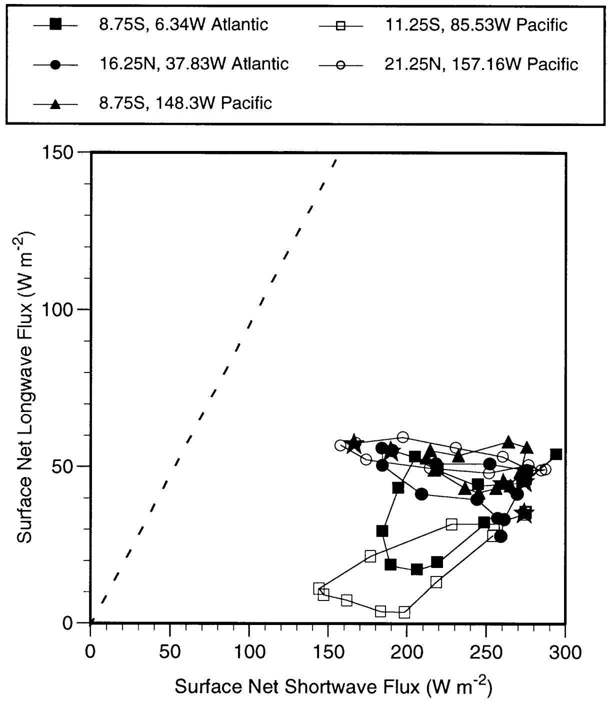

FIG. 6. Annual trajectory of NLW and NSW at surface for low-latitude ocean regions. Jan is indicated by ★ for each site.

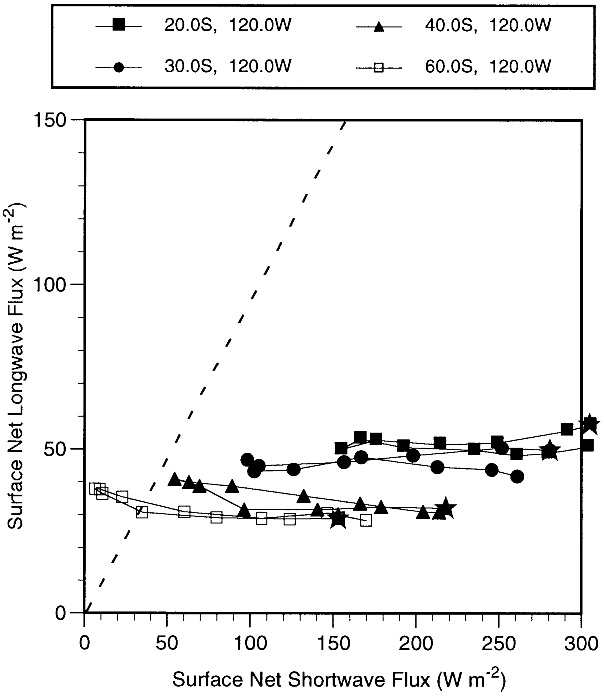

FIG. 7. Annual trajectory of NLW and NSW at surface for high-latitude ocean regions. Jan is indicated by ★ for each site.

NSW increases. In the extratropical oceans the seasonal temperature change and the accompanying change of upward LW is small compared to the changes of cloud forcing that cause this decrease of NLW.

4. Climate classification

The examination of the trajectories of various climatological regions indicates that the annual mean and range of the NSW and NLW are closely tied to the climatological characteristics of the surface. These relationships are now developed in terms of the climate classification method of TH80. Table 1 lists the climate classes of Trewartha and Horn for land in the left column. Figure 8 is a map of climate classifications reproduced from TH80. We examined maps of parameters that describe various features of the yearly cycle and evolved criteria that seemed physically reasonable and that produced agreement with the TH80 classification. These criteria are listed in the right column of Table 1 and are in fact simpler than our initial expectations. They are not considered to be unique as there are many aspects of the yearly cycle that are closely tied to the climate. First land regions are considered, followed by ocean regions.

a. Climate classes of land regions

Figure 9 is a map of annual-mean NLW. Comparison of Figs. 8 and 9 shows that the NLW of deserts are larger than those of other regions examined. Desert regions have annual-mean NLW greater than 90 W m^{-2} and steppe or semiarid regions have annual-mean NLW between 70 and 90 W m^{-2}. Other land regions have annual-mean NLW less than 70 W m^{-2}.

Figure 10 is a map of annual-mean NSW at the surface. Comparison of Fig. 10 with Fig. 8 shows that over land the annual-mean NSW contours for appropriate values correspond to the climate class boundaries for polar, boreal, and temperate regions. The annual-mean insolation at TOA is a function of latitude only. The boundaries for these climate classes are primarily zonal but change with longitude due to cloud cover and surface effects. The annual-mean NSW values that delineate these boundaries are listed in Table 1 for land regions. Figure 11 shows graphically these criteria for classification of climate of land regions. The axes of Fig. 11 are NSW and NLW and are similar to those of Figs. 2–7.

Distinguishing tropical and subtropical land regions requires information besides annual-mean NLW and NSW. Figures 2–5 show that for the few sites examined, the land regions in the Tropics have very little variation of NSW throughout the year, but in the subtropics the NSW varies significantly more. Figure 12 is a map of annual range of NSW and shows that subtropical land regions have an annual range of NSW greater than 100 W m^{-2} and tropical land regions have annual range of NSW less than 100 W m^{-2}.

Finally, a criterion is needed to distinguish between

TABLE 1. Climate classification by Trewartha and Horn for land and corresponding SRB criteria. Units are W m^{-2}. NSW and NLW are annual-mean values in this table. RSW denotes annual range of NSW flux.

A. Tropical:	NSW > 140, NLW < 70, and RSW < 100
Tropical wet (rain forest)	tropical and NLW < 50
Tropical wet and dry (savanna)	tropical and NLW > 50
B. Dry:	
Desert	NLW > 90
Steppe	70 < NLW < 90
C. Subtropical	NSW > 140, NLW < 70, and RSW > 100
D. Temperate	100 < NSW < 140 and NLW < 70
E. Boreal	50 < NSW < 100 and NLW < 70
F. Polar:	0 < NSW < 50 and NLW < 70
Ice cap	
Tundra	

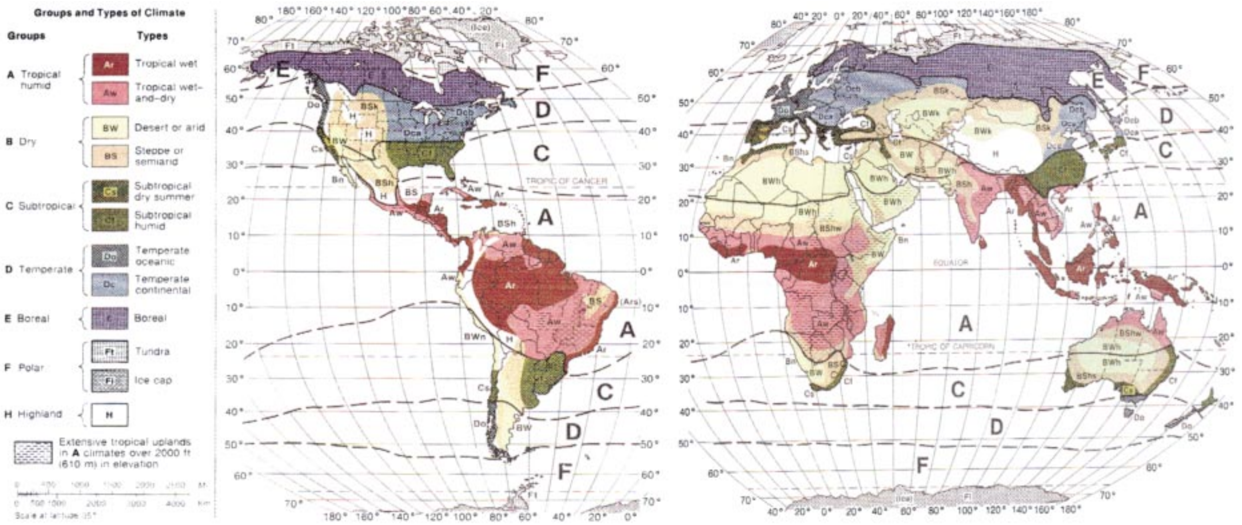

FIG. 8. Climate classification map of Trewartha and Horn (1980), *Introduction to Climate.* Reproduced by permission from McGraw-Hill, publisher.

tropical wet (rain forest) and tropical wet and dry (savanna) regions. Comparison of Figs. 8 and 9 shows that tropical wet regions have annual-mean NLW less than 50 W m^{-2}. This is because frequent cloud cover and high humidity are present throughout the year. The tropical wet and dry regions are marked by periods of dry weather broken by an annual or semiannual monsoon, so that the weather changes from tropical dry (desert) to tropical wet (rain forest). This change is accompanied by a large change in NLW from a high value of a desert to a low value of a tropical wet region, so that the annual-mean NLW is greater than 50 W m^{-2} for the

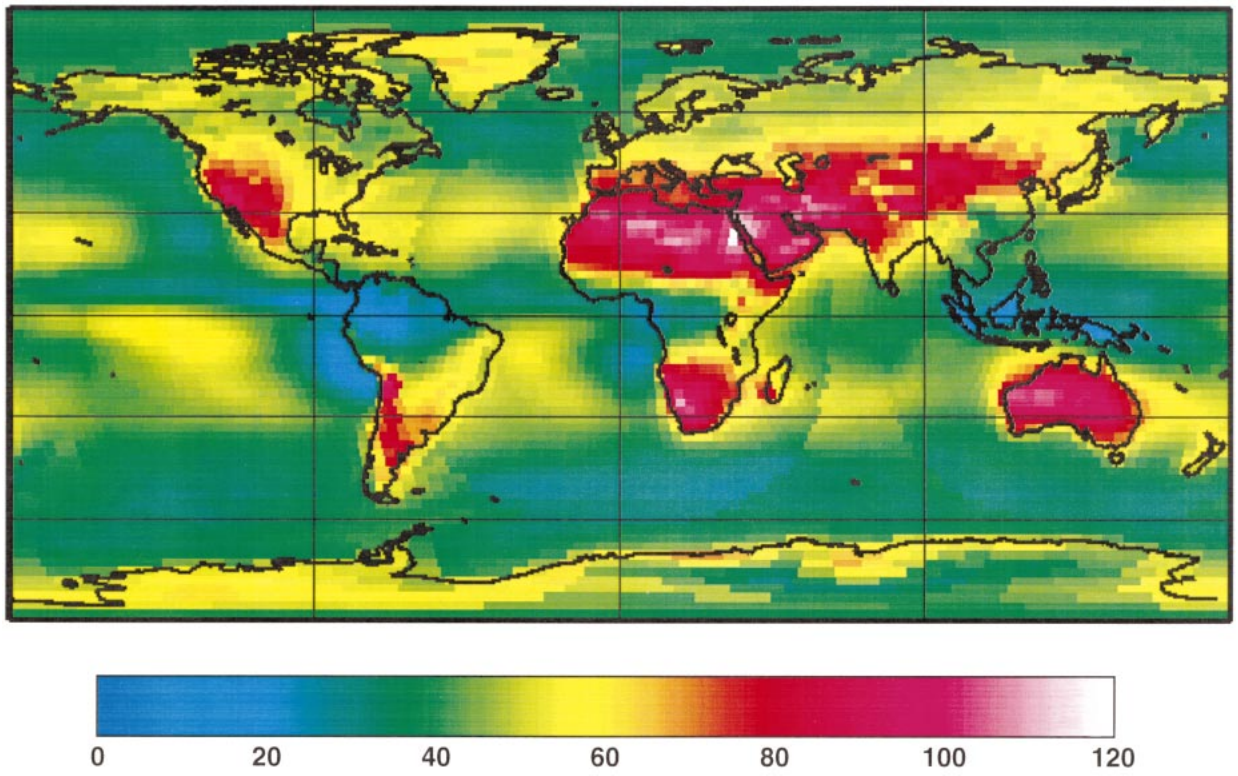

FIG. 9. Map of annual-mean NLW radiation flux.

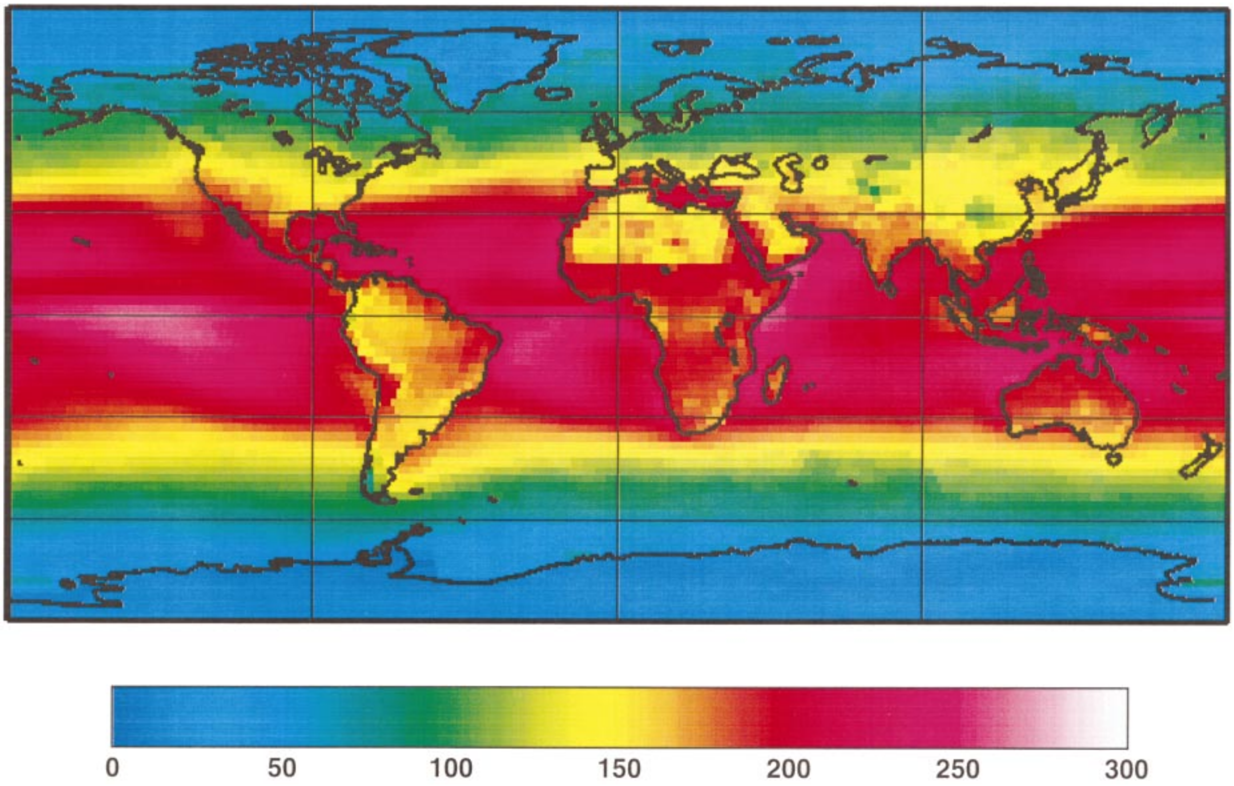

FIG. 10. Map of annual-mean NSW radiation flux.

wet–dry regions. Figure 13 shows graphically the criteria for distinguishing tropical and subtropical land regions. The abscissa is annual range of NSW and the ordinate is annual-mean NLW. The annual range of insolation at TOA is a function of latitude only, but the annual range of NSW varies with longitude due to cloud clover and surface effects.

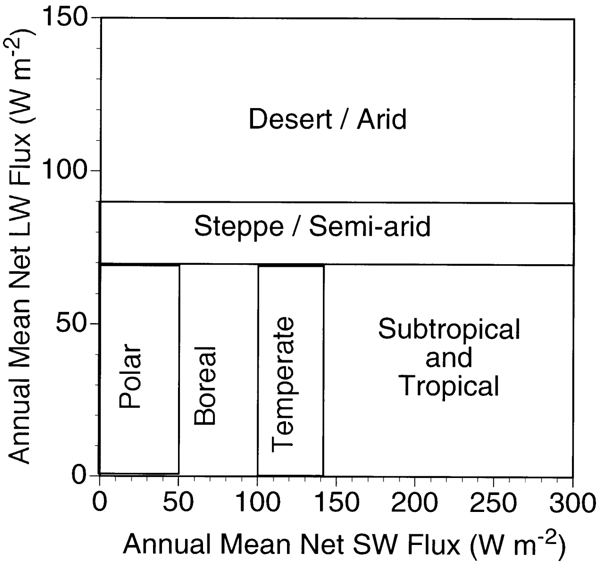

FIG. 11. Criteria for classification of climate of land regions.

b. Climate classes of ocean regions

An examination of the yearly cycles of ocean regions showed that NLW is small and does not vary much during the year. However, outside the Tropics the NSW varies over a large range. A comparison of Figs. 8 and 10 shows that as with land, one may select an annual-mean NSW value for which the contour corresponds quite closely to a climate class boundary for several ocean climate classes. These are listed in Table 2 as in Table 1. Figure 14 shows these criteria; its abscissa is annual-mean NSW. The polar and temperate regions separate nicely but as with land, another descriptor is required to distinguish between tropical and subtropical ocean regions. As with land, annual range of NSW was found to be suitable. For ocean, the annual range of NSW is less than 140 W m^{-2} for tropical and greater than 140 W m^{-2} for subtropical oceanic regions. Thus, the ordinate for Fig. 14 is the annual range of NSW.

Climate classification schemes are typically land oriented and do not usually include the intertropical convergence zones (ITCZ) and South Pacific convergence zone, which are prominent in radiation maps. These regions appear as tropical but with annual-mean NSW less than 210 W m^{-2}. With these criteria the eastern ocean stratus regions also appear. These are readily distinguished by their locations over the eastern parts of the oceans outside the Tropics. There is a gap between temperate ocean and ocean with convergence/stratus,

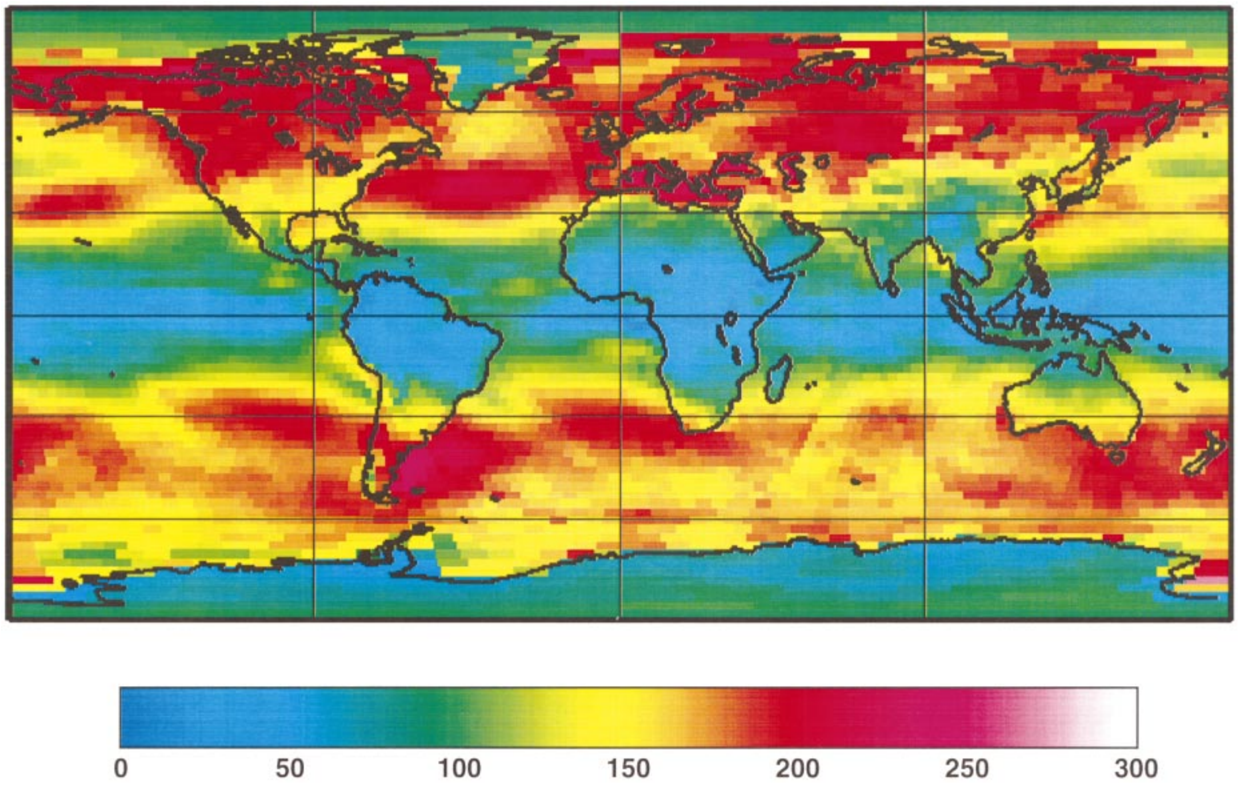

FIG. 12. Map of annual range of NSW radiation flux.

that is, there are no ocean regions with annual-mean NSW between 150 and 170 W m^{-2} and annual range of NSW less than 150 W m^{-2}. Subsidence regions over land, that is, desert and steppe, are distinguished by their large NLW (and extreme temperatures). For ocean regions with subsidence, the interaction between surface and atmosphere is totally different and ocean subsidence regions are not delineated in this classification (or others referenced).

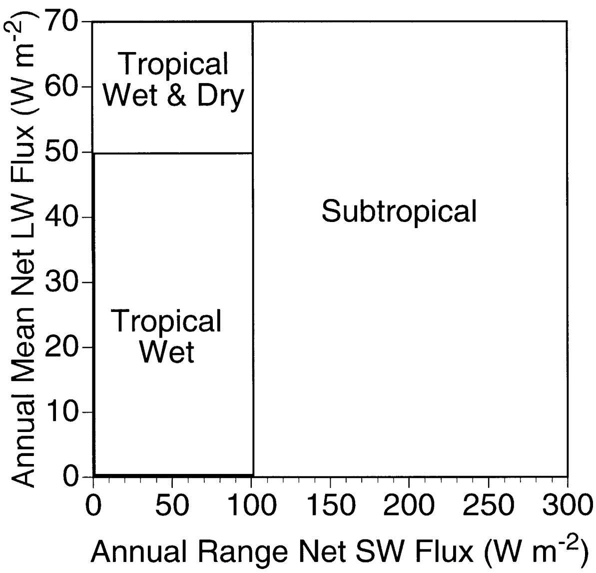

FIG. 13. Criteria for distinguishing tropical and subtropical land regions.

c. Climate classification map

Application of these criteria, depicted in Figs. 11 and 13 for land and Fig. 14 for ocean, to each region produces the climate classification map of Fig. 15. This map compares well with the climate classification map of TH80, shown in Fig. 8. The thresholds for the various criteria were chosen to match the boundaries between the climate classes of the TH80 map. TH80 in turn selected temperature and precipitation criteria to match the climate classification boundaries of Koeppen-Geiger which were based on plant types.

TABLE 2. Climate classification by Trewartha and Horn for ocean and corresponding SRB criteria. Units are W m^{-2}. NSW and NLW are annual-mean values in this table. RSW denotes annual range of NSW flux.

A. Tropical	NSW $>$ 210 and RSW $<$ 140
B. Convergence and stratus*	170 $<$ NSW $<$ 210 and RSW $<$ 140
C. Subtropical	NSW $>$ 150 and RSW $>$ 140
D. Temperate	80 $<$ NSW $<$ 150
F. Polar	0 $<$ NSW $<$ 80

* Not a class under Trewartha and Horn.

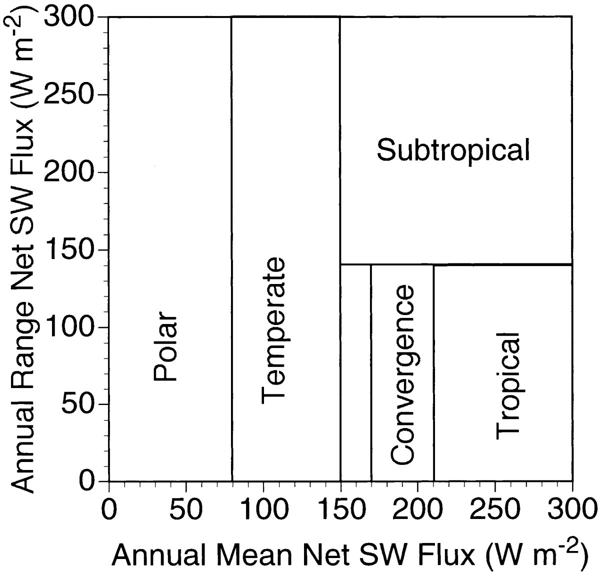

FIG. 14. Criteria for classification of climate of ocean regions.

5. Histograms

In Figs. 2–7, the yearly cycles of a few regions were examined in the SRB hodograph. In order to describe the totality of 6596 regions (i.e., grid boxes) it is necessary to use quantitative descriptors that can be summarized statistically. This section presents some statistical descriptions of the SRB divided into climate classes and types as in section 3c.

The first measures used to describe the figure are its centroid values, that is, its annual-mean NSW and NLW. Figure 16 is a two-dimensional histogram in the same format as Fig. 11 for the criteria for classification of land regions. Except for the Tropics and subtropics, the annual-mean NLW for all regions are tightly clustered within their climate class. The temperate, boreal, and polar regions all have annual-mean NLW near 50 W m^{-2}. Although there are desert and tropical wet–dry regions with annual-mean NSW exceeding 200 W m^{-2}, there are no regions with annual-mean NSW exceeding 220 W m^{-2}. Steppe regions have a wide range of annual-mean NSW. The reason for this wide range is that this class covers a broad range of extratropical latitudes and

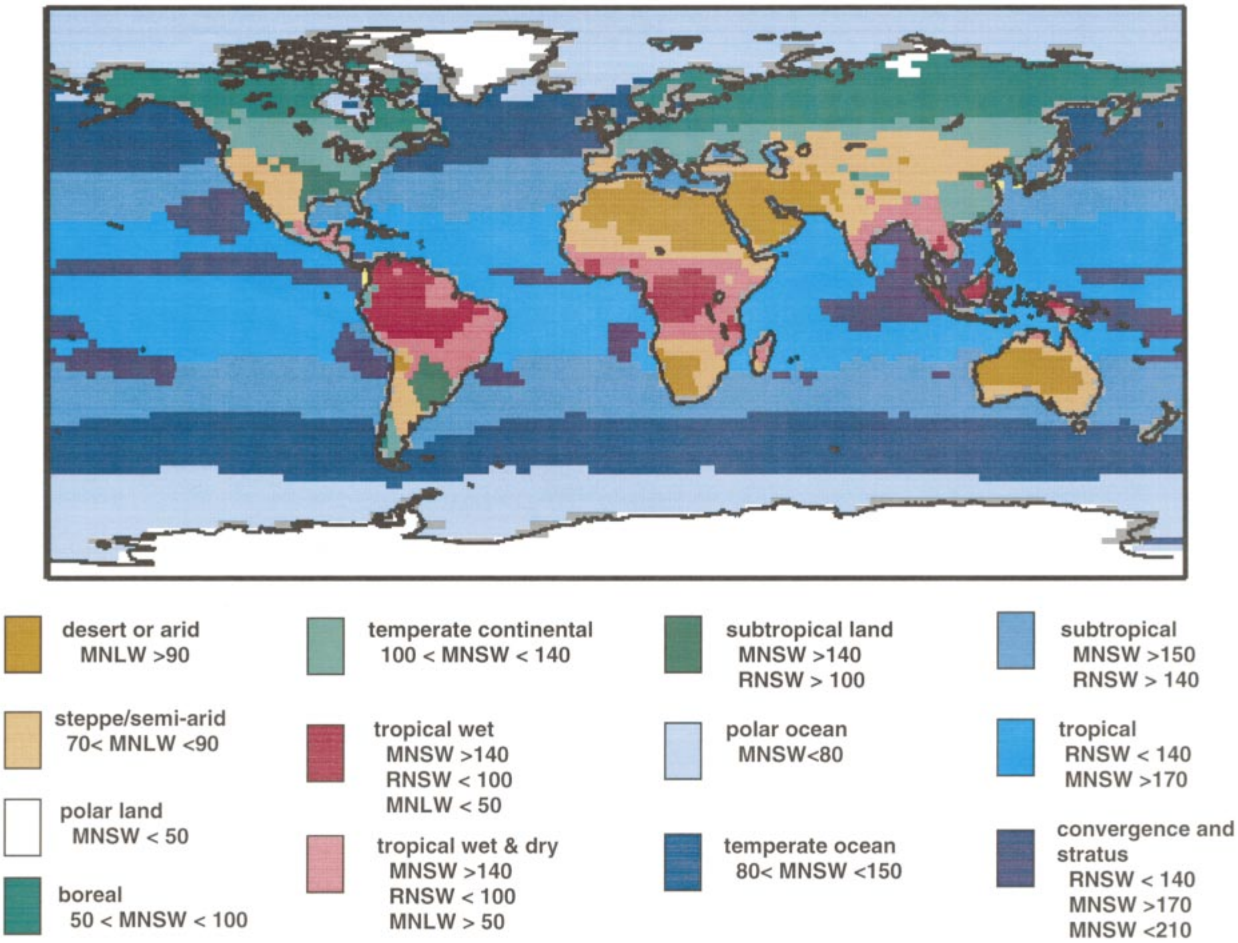

FIG. 15. Climate classification map based on SRB.

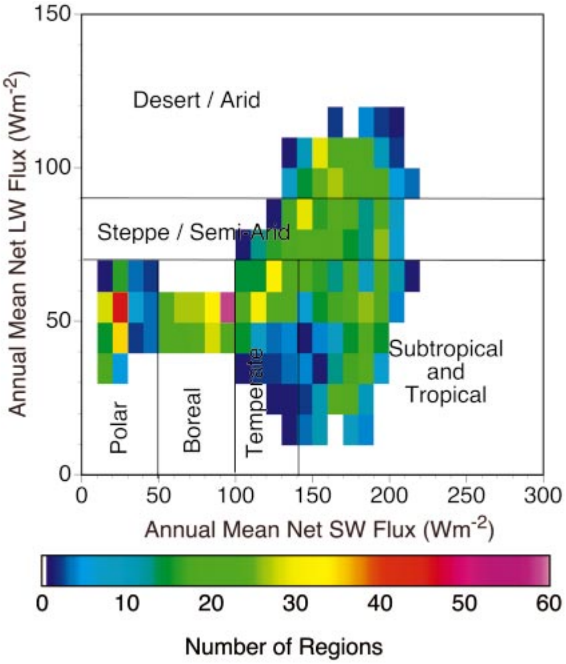

FIG. 16. Two-dimensional histogram of number of regions as function of annual-mean NLW and annual-mean NSW for land regions.

includes highland steppes and regions that are in the rain shadow of mountain ranges.

Figure 17 is a similar plot for ocean regions. Even more than with land, ocean regions are tightly clustered in terms of annual-mean NLW within their portion of

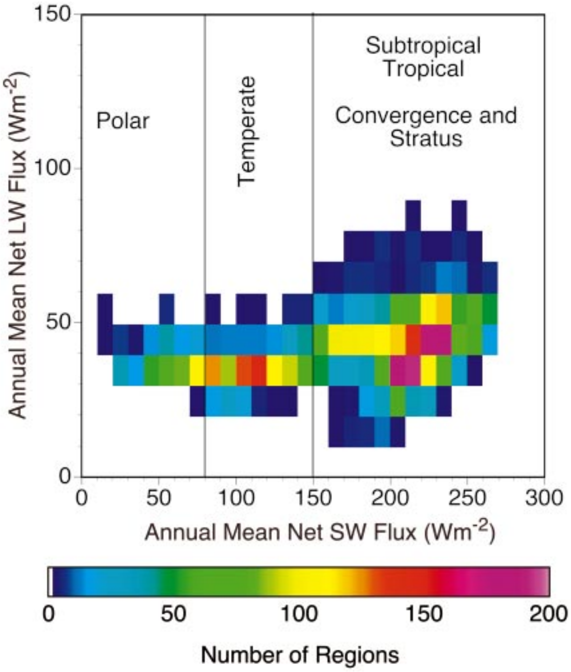

FIG. 17. Two-dimensional histogram of number of regions as function of annual-mean NLW and annual-mean NSW for ocean regions.

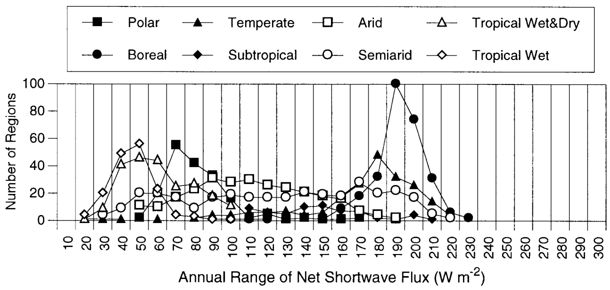

FIG. 18. Histogram of annual range of NSW flux for land regions.

the domain. The temperate and polar regions of the ocean have annual-mean NLW mostly between 30 and 40 W m^{-2}, with outliers down to 20 and up to 60 W m^{-2}. The narrowness of this range of annual-mean NLW is due to an interaction between the sea surface and the atmosphere. Likewise, the narrow range of annual-mean NLW for temperate, boreal, and polar land regions is due to an air–surface interaction.

One aspect of the variability of a region during the year is described in part by the annual range of its NSW, which is the driving force for the system. Figure 18 shows the histograms for annual ranges of NSW for the various climate classes. Boreal and temperate regions have large annual ranges of NSW. Tropical wet and tropical wet–dry regions have the smallest annual ranges of NSW. Steppe (semiarid) has a broad distribution of annual range of NSW. This reinforces the fact that there is a wide variety of conditions that result in a region being semiarid.

Figure 19 shows histograms of the annual range of NLW for land regions. For tropical wet–dry regions the annual ranges have a great variety, from small to quite large, with a median range of 55 W m^{-2}. This large variability is due to the change with the rainy season from desertlike conditions. Tropical wet regions have small annual ranges, with a median of 35 W m^{-2}. Boreal, temperate, and tropical wet regions have small ranges of NLW, with median ranges of 30 W m^{-2}. Desert and steppe regions have a median range of 45 W m^{-2}.

Except for the tropical wet–dry class, the annual range of NLW is small compared to the range of NSW. Even though the upward and downward longwave flux

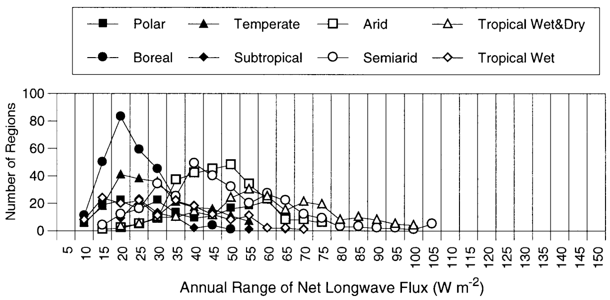

FIG. 19. Histogram of annual range of NLW flux for land regions.

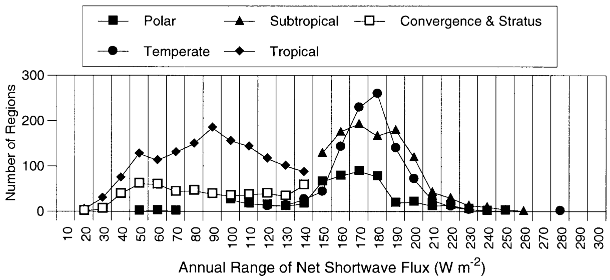

FIG. 20. Histogram of annual range of NSW flux for ocean regions.

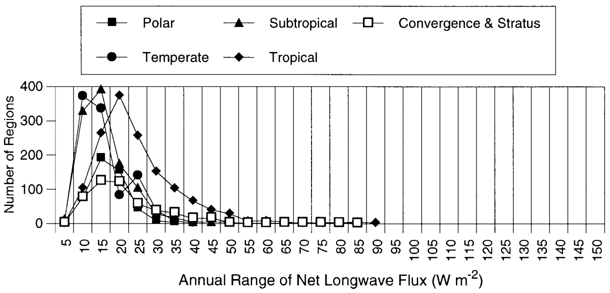

FIG. 21. Histogram of annual range of NLW flux for ocean regions.

components vary considerably, the NLW has a much smaller variation. The relatively small range of NLW compared to that of NSW demonstrates that the surface is strongly coupled to the atmosphere, through longwave radiative exchange and boundary layer processes. However, the range of NLW in temperate, boreal, and polar regions is large enough (10–50 W m^{-2}) that the small range of annual-mean NLW must be due in large part to averaging over the annual cycle.

Figure 20 shows histograms of the range of NSW over oceans. For polar, temperate, and subtropical oceans the peaks of the histograms of annual range of NSW are greater than 160 W m^{-2}, whereas the median of the annual range of NSW for tropical, convergence, and stratus oceanic regions is less than 90 W m^{-2}. The subtropical ocean is distinguished from the tropical, convergence and stratus zones by the criterion that the annual range of NSW is greater than 140 W m^{-2} for subtropical ocean and less for tropical, convergence, and stratus ocean regions.

Figure 21 shows histograms of the annual range of NLW for ocean regions. The median ranges of the polar, temperate, and subtropical oceanic regions are below 20 W m^{-2} but are larger for tropical, convergence, and stratus ocean regions. The insensitivity of the NLW to NSW of polar, temperate, and subtropical ocean can be attributed to the immense heat-storage capacity of the ocean and the close coupling of longwave radiative heating between the surface and atmosphere. In the tropical and convergence regions, the sea surface temperature and the atmospheric temperature are quite constant. The variations of the NLW of the tropical, and low-latitude convergence, and stratus ocean regions are primarily due to cloud variations with the yearly cycle. In particular, for a region covered by the ITCZ, the NLW will be low. Regions to the north and south will be subsidence regions, with low cloud and humidity, hence have large NLW. As the ITCZ moves north and south with the sun during the year, a region will have a large annual range of NLW as the condition above it changes from ITCZ to subsidence. This is the maritime equivalent of the tropical wet–dry class for land.

6. Discussion

It has been demonstrated that the trajectory of the annual cycle of the NLW and NSW is a characteristic of the climate of a region. Surface radiation is an agglomerate of temperature, humidity, and clouds. It is a component of the highly complex and tightly coupled climate system and as such is an indicator and driver of the state of the system. As a result, the climate class of a region can be found from very simple measures of the yearly cycle of NLW and NSW. Haurwitz and Austin (1944) and subsequent authors explain climatology in terms of air masses. These air masses in the mean have specific SRB properties. We have considered here only the major climate groups and types and have not attempted to refine the classification into subdivisions.

Precipitation is a very important component of climate and with temperature is the basis of the climate classification of TH80. Although precipitation is not explicitly considered here, humidity and cloudiness are strong drivers of SRB components. Thus, regions of high (low) precipitation have high (low) cloudiness and humidity and concomitant low (high) NLW.

Likewise, orography has a major influence on the climate of a region but is not explicitly considered here. The same considerations apply in regard to orography as for precipitation. TH80 include highlands as a climatological type. In the present study using only SRB, these regions appear as steppe (semiarid). The Eurasian steppes are largely in the rain shadow of the Himalayan and Caucasus Mountains. In North and South America the regions that are classed as steppe are likewise in the rain shadow of the Rocky or Andes Mountains. The low humidity over these regions results in the NLW being large so that the regions are steppe.

The classification of the regions in terms of climate brings order to the variety of annual cycles of SRB that have been noted and helps to explain them. Within each climatological class there are parameters that are characteristic of the class in addition to those selected here as distinguishing criteria. The SRB hodographs show interesting properties and behaviors, for example, the shape, the area enclosed within the trajectory, or its direction (clockwise or counterclockwise) raise a number of questions. Why are the SRB hodographs for temperate, boreal, and steppe and polar so linear? Why do the SRB hodographs for deserts enclose such a large area? The explanations for such questions involve not only the radiative interchange between the surface and the atmosphere but also convective transfer within the planetary boundary layer and variations of the large-scale circulation. The relative importance of the mechanisms in a region depends on its climate class. Addressing these aspects of the yearly SRB cycles will require further investigations.

TH80 point out that the boundaries between climate classes and types are not fixed, but can move from year to year with extended drought to plentiful rainfall over an extended period. The sharpness of these boundaries may be related to the interannual variability of radiation in the border regions. Also, the criteria established here have the potential to provide a mechanism for stating on the basis of satellite data whether a variation lasting for a year or more has caused the climate class of a region to change. For example, the Sahel is subject to extended drought periods lasting for years. In a drought year, the transition from a desertlike region to a region with convection would not occur. Another example of climate class change and SRB is the effect of carbon dioxide increase. The increase of carbon dioxide must have an effect on the boundaries between climatological types, both geographically and in terms of the parameters that are used by the criteria presented here. These changes would depend on the movement of subsidence zones and changes of precipitation patterns, all of which are coupled with the SRB. In order to predict these changes, a model including biospheric, atmospheric, and perhaps oceanic components is required.

This study only considered the domain of NLW–NSW at the surface. Other domains to be considered are net longwave–net shortwave radiation at the top of the atmosphere. Also, the domain of study need not be restricted to two independent variables; however, even though the computer capacity exists, studying more than two variables simultaneously is still difficult conceptually.

7. Conclusions

This study has examined the surface radiation budget for regions with differing climates. The yearly cycles for various regions form a variety of curves in the net longwave–net shortwave plane. These curves have different shapes and positions in the plane that are shown to characterize their differing climates. Defining the climate class of the regions brings order to the SRB yearly cycles and helps to explain their features. Desert regions are distinguished by high NLW and high NSW, with a small net total radiation at the surface. Tropical wet regions have small annual cycles and NLW but high NSW. Tropical wet–dry regions (savanna) have large changes of NLW as the dry and wet seasons alternate, but small variations of NSW, which is large throughout the year. For midlatitude continental regions, the NLW increases as NSW increases. However, the NLW decreases slightly with increasing NSW in the extratropical oceans.

A set of criteria has been developed that compute the climate classification of a region based on the annual means and ranges of the surface net longwave and shortwave radiative fluxes. Deserts (arid) are characterized by an annual mean NLW greater than 90 W m^{-2} and steppe (semiarid) by annual-mean NLW between 70 and 90 W m^{-2}. Temperate, boreal, and polar land regions are delineated by appropriate annual-mean NSW values. Temperate and polar ocean regions are distinguished similarly. For temperate, boreal, and polar land, the annual-mean NLW is close to 50 W m^{-2}, even though the net LW has a range of 10–50 W m^{-2} during the year. Other criteria characterize tropical and subtropical classes. Additional classes of convergence zones and stratus stand out for the ocean regions in terms of surface radiation budget. The resulting climate classifications compare quite well with climate classifications based on other considerations. This correspondence of the SRB results with other classifications demonstrates the intimate relation between surface radiation budget and the climatology of a region. These relations may provide a method for detecting regional climate change by use of satellite data.

Acknowledgments. This work was supported by the CERES and Surface Radiation Budget programs of the Earth Science Enterprise of NASA through Langley Research Center by Cooperative Agreement NCC1-405 to Virginia Polytechnic Institute and State University and Contract NAS1-19579, which supports Analytical Services and Material, Inc. Data were provided by the Atmospheric Sciences Data Center of NASA Langley Research Center.

REFERENCES

Barrett, E. C., 1974: *Climatology from Satellites.* Routledge, 418 pp.

Baum, B. A., and B. R. Barkstrom, 1993: Design and implementation of a prototype data system for Earth radiation budget, cloud, aerosol and chemistry data. *Bull. Amer. Meteor. Soc.,* **74,** 591–598.

Budyko, M. I., 1958: *The Heat Balance of the Earth's Surface.* U.S. Dept. of Commerce (U.S. Weather Bureau translation), 69 pp.

Charney, J. G., 1975: Dynamics of deserts and drought in the Sahel. *Quart. J. Roy. Meteor. Soc.,* **101,** 193–202.

Darnell, W. L., W. F. Staylor, S. K. Gupta, N. A. Ritchey, and A. C. Wilber, 1992: Seasonal variation of surface radiation budget derived from ISCCP-C1 data. *J. Geophys. Res.,* **97,** 15 741–15 760.

Gupta, S. K., W. L. Darnell, and A. C. Wilber, 1992: A parameterization for longwave surface radiation from satellite data: Recent improvements. *J. Appl. Meteor.,* **31,** 1361–1367.

——, N. A. Ritchey, A. C. Wilber, C. H. Whitlock, G. G. Gibson, and P. W. Stackhouse, 1999: A climatology of surface radiation budget derived from satellite data. *J. Climate,* **12,** 2691–2710.

Haurwitz, B., and J. M. Austin, 1944: *Climatology.* McGraw-Hill, 410 pp.

Koeppen, W., and R. Geiger, 1936: *Handbuch der Klimatologie.* Verlagsbuchhandlung.

Neelin, J. D., and I. M. Held, 1987: Modeling tropical convergence based on the moist static energy budget. *Mon. Wea. Rev.,* **115,** 3–12.

Ramanathan, V., 1986: Scientific use of surface radiation budget for climate studies. Position paper on Surface radiation budget for climate application, NASA Reference Publication RP-1169, 58–86.

Rossow, W. B., and R. A. Schiffer, 1991: ISCCP cloud data products. *Bull. Amer. Meteor. Soc.,* **72,** 2–20.

Sanderson, M., 1999: The classification of climates from Pythagoras to Koeppen. *Bull. Amer. Meteor. Soc.,* **80,** 669–673.

Terjung, W. H., 1970: Toward a climate classification based on net radiation. *Proc. Assoc. Amer. Geogr.,* **2,** 140–144.

Trewartha, G. T., and L. H. Horn, 1980: *An Introduction to Climate.* McGraw-Hill, 416 pp.